JACS
JOURNAL OF THE AMERICAN CHEMICAL SOCIETY
Article
pubs.acs.org/JACS

Intracellular CO Release from Composite of Ferritin and Ruthenium Carbonyl Complexes

Kenta Fujita,[†] Yuya Tanaka,[‡] Takeya Sho,[†] Shuichi Ozeki,[†] Satoshi Abe,[†] Tatsuo Hikage,[§] Takahiro Kuchimaru,[†] Shinae Kizaka-Kondoh,[†] and Takafumi Ueno*[,†]

[†]Department of Biomolecular Engineering, Graduate School of Bioscience and Biotechnology, Tokyo Institute of Technology, Nagatsuta-cho 4259-B55, Midori-ku, Yokohama 226-8501, Japan

[‡]Chemical Resources Laboratory, Tokyo Institute of Technology, R1-27, 4259 Nagatsuta-cho, Midori-ku, Yokohama 226-8503, Japan

[§]High Intensity X-ray Diffraction Laboratory, Nagoya University, Furo-cho, Nagoya, 464-8603, Japan

Supporting Information

ABSTRACT: Protein cages have been utilized as templates in the development of biomaterials. Here we report protein engineering of the ferritin (Fr) cage for encapsulating carbon monoxide releasing molecules (CORMs) and release of CO gas which serves as a cell signaling molecule. The protein cages enable us to increase the half-life for CO release, providing a release rate that is 18-fold slower than the rate of a typical CORM, $Ru(CO)_3Cl(glycinate)$ (CORM-3). Moreover, the uptake ratio of the composite is about 4-fold greater than that of CORM-3. We found that these effects enhance the activation of nuclear factor κB 10-fold higher than CORM-3. The protein cage of Fr thus provides the basis for new CORMs that can be used for in vitro cell research.

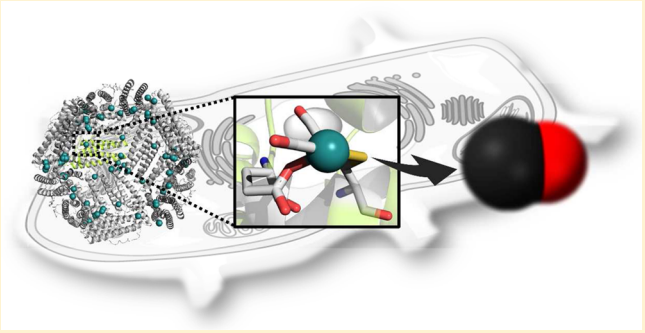

INTRODUCTION

Protein cages composed of multimeric protein assemblies have been used for development of biomaterials.[1−4] Metal complexes and nanoparticles are encapsulated within the inner cavities in restricted numbers, coordination structures, and size distributions.[2,4] These composites can function as catalytic, magnetic, and photonic materials for biomedical applications.[3,4] Recently, many researchers have been applying these effects in development of drug delivery systems because the activities and stabilities of the materials can be retained within the cage after delivery into living cells.[5−14] For example, Douglas and co-workers utilized the ferritin protein cage as a carrier of iron oxide nanoparticles in efforts to deliver iron oxide to living cells.[12] Metal complexes such as cisplatin (a chemotherapeutic agent) and Gd complexes (MRI imaging reagents) have been encapsulated in Fr and delivered into living cells.[8,9] A zinc phthalocyanine encapsulated cowpa chlorotic mottle virus was synthesized for use in photodynamic therapy.[7] Further development of protein cages with metal complexes is required not only for fundamental research but also for applications in biomedical sciences.

Organometallic complexes have recently attracted attention as biomedical reagents, such as metal-based drugs and imaging materials in living cells.[15,16] Metal carbonyl complexes known as carbon monoxide releasing molecules (CORMs) have been utilized to deliver carbon monoxide (CO) to living cells.[17−21] This exogenous CO acts as an intracellular signaling molecule to produce cytoprotective effects that counteract inflammation, proliferation, and apoptosis.[19,20] Motterlini and co-workers developed useful CO therapeutic tools with $[Ru(CO)_3Cl_2]_2$ (CORM-2) and $Ru(CO)_3Cl(glycinate)$ (CORM-3) which can release CO into mammalian cells.[17] Many organic ligands have been synthesized to modulate the CO release properties because CO is expected to be released from the complexes by a ligand exchange reaction with intracellular electron-donating molecules such as glutathione.[22] However, the fast degradation and relatively poor uptake ratio of CORMs into living cells have prevented them from being used in investigations involving CO delivery.[17,19] Because of the problems encountered with delivery of CO into cells using CORMs, it is difficult to clearly define the effects of CO in signaling pathways.[22−24] Significant re-engineering of CORM carriers is needed to overcome these problems. Romão and co-workers reported CORMs based on protein−$Ru(CO)_2$ composites.[23,24] However, delivery of these molecules to living cells has not been achieved.[23,24] Although a fast ligand exchange reaction and cytotoxicity were suppressed by encapsulating CORM-3 within micelle compounds, sufficient delivery of CO has not been addressed by this system.[22] We recognized that the Fr protein cage provides the possibility to resolve both of these problems simultaneously because a previous report showed that Fr has the capability to

Received: August 29, 2014
Published: October 28, 2014

   dx.doi.org/10.1021/ja508938f | J. Am. Chem. Soc. 2014, 136, 16902−16908

encapsulate metal nanoparticles that would reduce their cytotoxicity.[5] In addition, Fr undergoes cell surface receptor-mediated endocytosis, which would improve uptake ratio of metal nanoparticles.[5] Therefore, we chose to investigate whether Fr can be used as an intracellular CORM delivery carrier.

Here we describe the preparation of composites of ferritin (Fr) with CORM (Fr-CORM) and the use of these composites in investigations of intracellular CO releasing properties (Figure 1). Fr includes 24 subunits and has an outer diameter of 12 nm

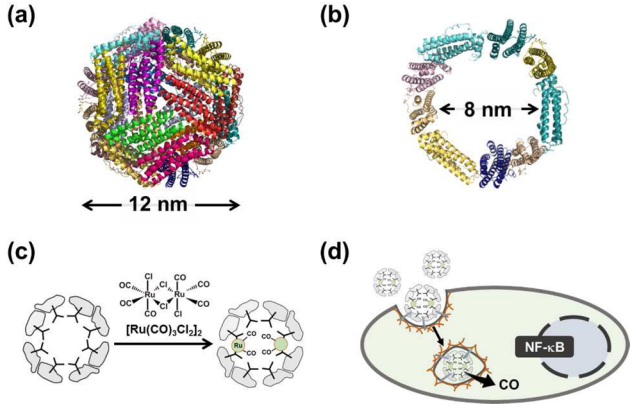

Figure 1. CO releasing protein cage for induction of intracellular signaling. Crystal structure of apo-ferritin: (a) the whole structure with 24-mer, (b) the cross section drawing of the inner cavity (PDB code 1DAT), (c) schematic representation of recombinant L-chain apo-ferritin from horse liver (apo-rHLFr) with Ru carbonyl complexes (RuCO·apo-rHLFr (**1**)). $[Ru(CO)_3Cl_2]_2$ (CORM-2) is incorporated into the apo-rHLFr cage, then bound to amino acid residues exposed on the interior surface with the appropriate coordination structure. (d) Endocytic uptake of **1** and NF-κB activation in HEK293/κB-Fluc cell by the CO release. The composite can penetrate into living cells with endocytosis, then release CO gas to activate NF-κB.

and an inner diameter of 8 nm (Figure 1a and Figure 1b).[25] Fr can enter the cell via an endocytic pathway through a specific cell surface receptor.[11] In past studies, we succeeded in encapsulating organometallic complexes into the Fr cage to provide composites with high stability and large accumulation numbers of organometallic complexes.[26−30] Catalytic reactivity of the complexes was controlled by specific amino acid replacements within the cage.[26,27] Fr-CORM composites are expected to be delivered into the cells while retaining their original carbonyl coordination structures within the cage. We found that the composites activate nuclear factor κB (NF-κB) which plays an important role in expression of cellular proteins via a signaling pathway that is regulated by CO.[31] The use of Fr as a CORM carrier provides a new gas delivery system based on protein cages.

RESULTS

A composite of recombinant L-chain apo-ferritin from horse liver (apo-rHLFr) with Ru carbonyl complexes (RuCO·apo-rHLFr (**1**)) was prepared by adding a DMF solution of $[Ru(CO)_3Cl_2]_2$ (CORM-2) to a buffer solution of apo-rHLFr (50 mM Tris/HCl (pH 8.0), 0.15 M NaCl). A crystal structure of **1** was refined to 2.00 Å resolution. There are 72 Ru binding sites of Ru atoms identified at accumulation centers and 3-fold axis channels (Figure 2a and Figure 2b).[26−30] The Ru atoms at the 3-fold axis channel have less occupancy than at the

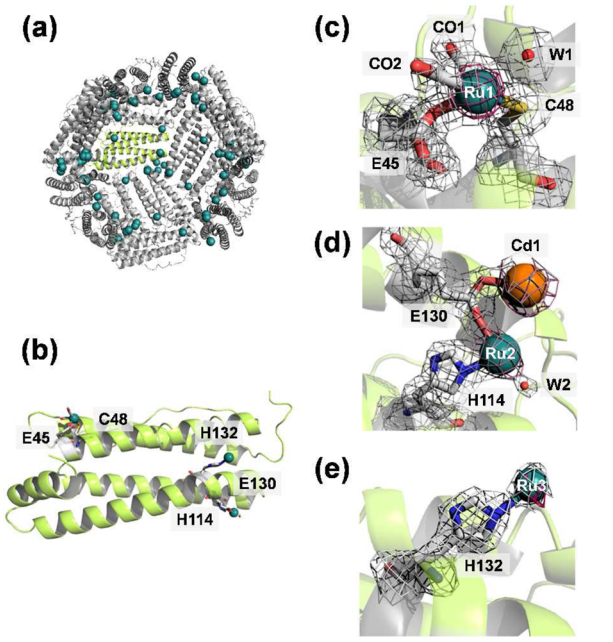

Figure 2. X-ray crystal structure of RuCO·apo-rHLFr (**1**): the whole structure consisting of the 24 protein monomers (a) and the monomer structure with Ru binding sites (b). The Ru coordination structures at the accumulation center (c), the 3-fold axis channel (d), and His132 site (e). Ru, Cd, O atoms of water molecules are shown as green, orange, red spheres, respectively. Anomalous difference Fourier maps at 4.0σ indicates the positions of Ru atoms shown as pink. The $2|F_o| - |F_c|$ electron density maps at 1.0σ are colored in gray.

accumulation center. At the accumulation center, an anomalous peak corresponding to a Ru atom (Ru1) was observed (Figure 2c). It coordinates to Oε of Glu45 and Sγ of Cys48 with bond lengths of 2.33 and 2.70 Å, respectively (Figure 2c). The CO ligands (CO1 and CO2) are coordinated to the Ru1 atom with bond distances of 1.80 and 2.10 Å, respectively. These distances of Ru1−O, Ru1−S, Ru1−C1, and Ru1−C2 bonds are in the typical range of Ru carbonyl complexes (Figure 2c).[23,32,33] The C1−Ru−C2 angle of 94.6° suggests that two carbonyl moieties are coordinated in a *cis*-$Ru(CO)_2$ structure to the Ru1.[23,33] These results indicate that the *cis*-$Ru(CO)_2$ structure is retained within the apo-rHLFr cage. The coordination structures of the CO ligands were confirmed by attenuated total reflectance infrared (ATR-IR) spectroscopy. Two peaks of carbonyl stretching frequencies were observed at 2038 and 1956 cm^{-1}, which were assigned to the *cis*-$Ru(CO)_2$ structure (Table 1).[23,24] At the 3-fold axis channel, the Ru2 atom was found to be coordinated to Nε of His114 and Oε of E130 with distances of 2.46 and 2.54 Å, respectively (Figure 2d). The Ru3 atom was

Table 1. Carbonyl Stretching Frequencies of Fr-CORM Composites and CORM-3[a]

composite	wavenumber, cm^{-1}
RuCO·apo-rHLFr (**1**)	2038, 1956
RuCO·apo-E45C/C48A-rHLFr (**2**)	2045, 1972
RuCO·apo-R52C-rHLFr (**3**)	2040, 1960
CORM-3	2137, 2072, 2058

[a]Measured by ATR-IR spectroscopy. Fr-CORM composites were dissolved in 50 mM Tris/HCl buffer (pH 8.0), and CORM-3 was dissolved in water.

dx.doi.org/10.1021/ja508938f | J. Am. Chem. Soc. 2014, 136, 16902−16908

found to be bound to Nε of His132 at a distance of 2.30 Å (Figure 2e). An anomalous peak of a Cd atom (Cd1) was confirmed to be located at the same position as that in apo-rHLFr.[34] The occupancy values of Ru2 and Ru3 atoms were lower (0.4 and 0.3, respectively) than that of Ru1 (0.8). This is one of the reasons why the number of Ru atoms estimated by the ICP-MS and BCA assay (48 ± 2) differs from that of the crystal structure (72) as reported previously for Pd·apo-rHLFr.[30,35]

The CO release properties of Ru carbonyl complexes can be modulated by coordination of ligands with different electronic properties because poor electron donors are expected to decrease the binding strength of CO ligands to Ru atom through back-donation.[17,18,36] On the basis of the crystal structure, apo-E45C/C48A-rHLFr and apo-R52C-rHLFr mutants were utilized to modulate the Ru−CO coordination by alteration of the electron donor character of cysteine and histidine residues.[28] The composites RuCO·apo-E45C/C48A-rHLFr (**2**) and RuCO·apo-R52C-rHLFr (**3**) were prepared under the same conditions used for **1** (see Supporting Information).

Crystal structures of RuCO·apo-E45C/C48A-rHLFr (**2**) and RuCO·apo-R52C-rHLFr (**3**) were refined to 1.92 and 1.82 Å resolution, respectively. The structure of **2** showed 96 anomalous electron densities within the cage (Figure 3a). The Ru atoms were found to be located at the accumulation center and the 3-fold axis channel (Figure 3b). The number of binding sites is different from the value estimated by ICP-MS and BCA assay (53 ± 5 Ru). The occupancies of the Ru atoms at the accumulation center (Ru4, 0.8; Ru5, 0.7) were found to be higher than that of the 3-fold axis channel and the His132 site (0.5 and 0.4) (Figure 3c). A thiolate-bridged dinuclear Ru cluster was formed at the accumulation center with a Ru4−Ru5 bond length of 2.71 Å and a Ru4−S−Ru5 bond angle of 74.9° as previously reported.[37] The Ru atoms were found to be coordinated to the bridged Sγ atom of Cys48 and the Nε atoms of His49 and His173, although the electron density of His173 was too low to fit to the model as observed in Ru(*p*-cymene)·apo-rHLFr composite.[28] At the 3-fold axis channel and His132, the Ru atoms were found to be bound to apo-E45C/C48A-rHLFr in a manner similar to that of **1** (Figure 2d, Table S2). Two peaks arising from the CO stretching frequencies of **2** were observed at 2045 and 1972 cm^{-1} (Table 1), although there were no electron density assignable to CO ligands in the crystal structure. These results suggest that **2** has *cis*-$Ru(CO)_2$ coordination structure similar to the coordination structure observed for **1** (Table 1).

The apo-R52C-rHLFr mutant was utilized to promote S,S-bidentate ligation at the accumulation center. A crystal structure of **3** showed 48 anomalous peaks corresponding to two Ru atoms (Ru6 and Ru7) at all of the accumulation centers within the cage (Figure 3d and Figure 3e). This accumulation number is essentially identical to the value estimated using the ICP-MS and BCA assay (45 ± 3). The occupancies of the Ru atoms were 0.7 and 0.7 for Ru6 and Ru7, respectively.

Ru6 and Ru7 were found to be bound to the Oε atom of Glu45 and the Sγ atom of Cys52, respectively, by a bridging ligation of Cys48 with appropriate distances (Figure 3f, Table S2).[33] The *cis*-$Ru(CO)_2$ coordination within **3** is presumed to arise from the CO stretching frequencies of **3** (2040, 1960 cm^{-1}) which are the same as the stretching frequencies for **1** and **2** (Table 1). There were no anomalous peaks at the 3-fold axis channel of **3**. The structure is different from that of **1** and **2** at the site. The reason will be clarified by further investigation.

The CO release properties of all of the Fr-CORM composites were evaluated using the myoglobin (Mb) assay in 10 mM PBS buffer (pH 7.4) in the presence of dithionite (7 mM) under Ar atmosphere (Table 2).[17,19] Conversion from deoxy-Mb to carbonmonoxy-Mb (MbCO) was calculated by following the previous procedure.[22] The CO release amount and half-life ($t_{1/2}$) were determined by fitting to first-order kinetics (Figure S1).

The amount of CO released from **1** per Ru was 0.08 ± 0.02, with a half-life ($t_{1/2}$) of 36.8 ± 0.3 min. The $t_{1/2}$ value is 18-fold

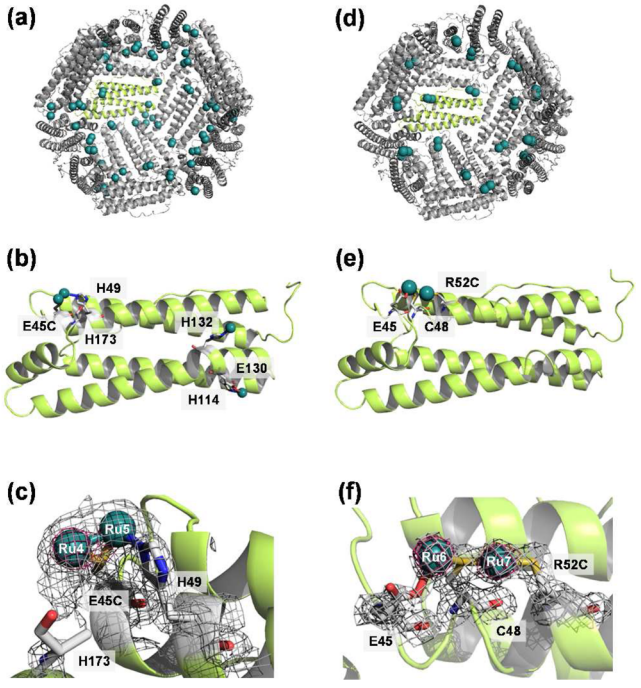

Figure 3. X-ray crystal structures of RuCO·apo-E45C/C48A-rHLFr (**2**) and RuCO·apo-R52C-rHLFr (**3**): the whole structure of **2** (a) and **3** (d), the monomer protein structure with Ru binding sites for **2** (b) and **3** (e), and the Ru coordination structures at the accumulation center of the monomer protein for **2** (c) and **3** (f). Coordinated Ru atoms are shown as green spheres. Anomalous difference Fourier maps at 4.0σ indicate the positions of Ru atoms shown as pink. The $2|F_o| - |F_c|$ electron density maps at 1.0σ are colored in gray. His173 was replaced with Ala residues because of the disordered electron densities of the side chains.

Table 2. Number of CO Equivalents Liberated Per Mole of Ru Atom and Half-Life ($t_{1/2}$) for CO Release from Fr-CORM Composites and CORM-3[a]

composite	equivalents of CO per Ru	$t_{1/2}$, min
RuCO·apo-rHLFr (**1**)	0.08 ± 0.02	36.8 ± 0.3
RuCO·apo-E45C/C48A-rHLFr (**2**)	0.16 ± 0.04	35.5 ± 0.3
RuCO·apo-R52C-rHLFr (**3**)	0.08 ± 0.02	36.7 ± 0.4
CORM-3	0.61 ± 0.03	2.2 ± 0.4

[a]All Fr-CORM composites and CORM-3 were added to the Mb solution (10 mM PBS buffer (pH 7.4)) containing dithionite (7 mM) under Ar atmosphere. Conversion of Mb to MbCO was traced using a UV−vis spectrometer. After the calculation of the equivalents of CO/Ru, $t_{1/2}$ was determined by fitting to first-order kinetics. All determinations were carried out at least in triplicate.

dx.doi.org/10.1021/ja508938f | J. Am. Chem. Soc. 2014, 136, 16902−16908

longer than that of CORM-3. The released amount of CO is 8-fold lower than that of CORM-3. The decrease comes from the stability of the *cis*-$Ru(CO)_2$ complex as described previously.[24] The 2-fold increase of the amount of CO was confirmed for **2** compared to the value of **1** with almost the same $t_{1/2}$ value (0.16 ± 0.04, 35.5 ± 0.3 min). The CO release properties of **3** are comparable to the values of **1**. Gel permeation chromatography (GPC) experiments showed that the whole structure of **2** was retained after incubation with dithionite for 100 min in the absence of Mb (Figure S2). In the Mb assay, an excess amount of dithionite was thought to be a trigger of CO release.[38] To confirm the mechanism, oxyhemoglobin (oxy-Hb) was used for CO release assay as previously reported.[38] In the absence of dithionite, there was no change in the spectra of oxy-Hb reacted with **2** for 100 min (Figure S3). Thus, dithionite can induce the CO release without any influence on the cage structure of **2**.

Cellular uptake of L-chain Fr is known to occur via receptor-mediated endocytosis.[39] Uptake of Fr-CORM composites into HEK293/κB-Fluc cells was observed by confocal microscopy for **1** modified with ATTO (ATTO-**1**) (see Experimental Section and Figure S4). The cage structure of rHLFr was retained in the cellular environment because GPC experiments revealed that the ATTO-**1** composite showed a peak assigned to the whole Fr cage after the cellular incubation for 12 h (Figure S5). The uptake ratio of Ru atoms into the cells was determined by inductively coupled plasma mass spectrometry (ICP-MS) (Figure 4). HEK293/κB-Fluc cells incubated with

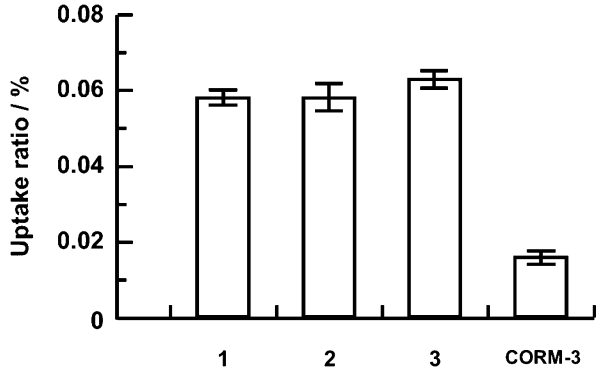

Figure 4. Uptake efficiency of Ru atoms of Fr-CORM composites and CORM-3. Each sample was incubated for 12 h with HEK293/κB-Fluc cells at 37 °C under 5% CO_2. The final concentration of Ru atoms added into the cell of Fr-CORM composites was 10 μM except for CORM-3 (200 μM) because the content of CORM-3 was not detected at the same concentration for **1**−**3** (10 μM) because of the low uptake ability of CORM-3.The concentrations of cellular uptake Ru atoms were measured by ICP-MS. The average values of three wells for each sample are shown in this figure.

each Fr-CORM composite or CORM-3 for 12 h were collected as a pellet after removing excess Ru compounds in the medium. The cell pellet was lysed with 10% Tween 20 to measure the concentration of Ru in the cell lysate by ICP-MS (see Experimental Section).[40] The uptake ratios determined for **1**, **2**, **3**, and CORM-3 were 0.058%, 0.058%, 0.063%, and 0.018%, respectively. Intracellular CO release from **2** was observed by using CO probe 1(COP-1) with confocal microscopy (Figure S6).[41] **2** could release CO inside the HEK293/κB-Fluc cells the same as for CORM-3.

The effect of CO released from the Fr-CORM composites on NF-κB activity was evaluated in HEK293/κB-Fluc cells which were modified for a luciferase assay because CO gas is known to activate NF-κB in the presence of tumor necrosis factor α (TNF-α).[42] The cells were stimulated with 1.0 ng/mL TNF-α after preincubation with the Fr-CORM composites for 1 h, and then they were incubated for 12 h. **1** and **3** were found to be capable of activating NF-κB with ∼4-fold increase compared to CORM-3 as shown in Figure 5. The activation of NF-κB by **2** was ∼2.5-fold higher relative to **1** and **3**.

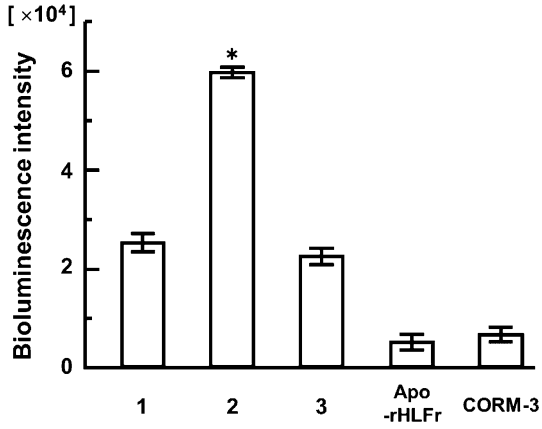

Figure 5. Bioluminescence intensity of luciferase reporter assay for evaluating the NF-κB activity of HEK293/κB-Fluc cells. The cells were preincubated for 1 h at 37 °C with **1**, **2**, **3**, and CORM-3. After the incubation, cells were stimulated by 1.0 ng/mL TNF-α, and then the cells were cultured for 12 h: (∗) $P < 0.05$ vs 0.1 M Na phosphate buffer added cells. All the data show subtracted bioluminescence intensity of the samples from that of the 0.1 M sodium phosphate buffer (pH 7.0) added cells. The experiments were performed three times, and the data represent the mean ± SEM.

In addition, **2** showed a concentration dependence of the activation, while CORM-3 did not have the same tendency (Figure S7a). A 3-(4,5-dimethylthiazol-2-yl)-2,5-diphenyltetrazolium bromide (MTT) assay indicated that the Fr-CORM composites were not cytotoxic for HEK293/κB-Fluc cells (Figure S8).

DISCUSSION

The results suggest that the Fr cage is a suitable CORM carrier for use in investigations of NF-κB activation by CO because of higher activation ability of the composites compared with reported CORMs. We expect that the activation of NF-κB is enhanced by three factors described below.

The first major factor enhancing activation of NF-κB is the extension of the half-life of CO release from each of the composites. The values are about 18-fold longer than that of CORM-3 regardless of the number of CO molecules released from the composites (Table 1). The *cis*-$Ru(CO)_2$ structure of each of the Fr-CORM composites is an important factor providing slow release as previously mentioned for a HEWL-CORM composite.[23,24] The proposed mechanism of release of CO from ruthenium carbonyl complexes is expected to include a ligand exchange reaction with dithionite under the conditions of the Mb assay.[38] In living cells, the reaction is thought to proceed by using intracellular electron donor ligands such as glutathione or cysteine which are present in the cytoplasm at millimolar concentrations.[22] Accessibility of the intracellular

dx.doi.org/10.1021/ja508938f | J. Am. Chem. Soc. 2014, 136, 16902−16908

ligands into the Fr cage is limited by the requirement of penetration through the 3-fold axis channels.[43] Thus, the slow release of CO from Fr-CORM observed with the Mb assay is expected to occur in HEK293/κB-Fluc cells. **2** showed concentration dependence for NF-κB activation (Figure S7a). However, CORM-3 did not show the same tendency. These results suggest that the slow CO release is more crucial for the activation by CO than uptake ratio of CORMs into living cells.

The second factor contributing to enhancement of activation of NF-κB is the increase of the amount of CO released from RuCO in apo-rHLFr (Figure 4). This effect was achieved by construction of a dinuclear RuCO structure at the accumulation center of **2**. The composite can release twice the amount of CO of **1** and **3** (Table 1). The dinuclear coordination structure in **2** is retained by ligation of Cys45, His49, and His173, due to the high flexibility of His173 at the C-terminus.[29] ATR-IR data show that the poor electron donor characteristics of His49 and His173 cause weaker back-donation to CO ligands bound to the Ru atoms than Glu45 or Cys52 in **1** or **3** (Table 1).[44] It is expected that the coordination structures are retained in living cells because the Fr cage structure is stable in living cells as shown in Figure S5. These results suggest that the amount of CO released from the Fr-CORM composites in living cells can be increased by introducing His coordination within the Fr cage.

The uptake ratio of the Fr cage is the third advantage as a CORM carrier. Cellular uptake of Fr is known to occur via receptor-mediated endocytosis.[40] The uptake ratio of micelle CORM (0.02%) is almost comparable with that of CORM-3, although the specific uptake mechanism has not been identified for micelle CORM and CORM-3.[22] The previously reported hen egg white lysozyme (HEWL)-CORM composite did not activate NF-κB because of less uptake ratio (Figure S7b).[23,45] It is revealed that CORMs in the Fr cages are able to deliver large amounts of CO into the cell with slow release rate to activate NF-κB.

■ CONCLUSIONS

We constructed Fr-CORM as new CORMs with proteins. The composites can serve as useful tools for activating NF-κB compared to CORM-3. The advantage of Fr as a CORM carrier is provided by (1) slow release of CO, (2) modulation of appropriate coordination structure of CORM in the cage, and (3) high uptake ratio into living cells. All three factors are modulated by protein engineering of Fr. The detailed mechanism of NF-κB activation is being further investigated with efficient CO delivery using the Fr cages. Thus, Fr-CORM can be applied as chemical tools to conduct extensive research on CO gas biology for clinical applications.

■ EXPERIMENTAL SECTION

Materials. All reagents were purchased from commercial suppliers and used without further purification. $Ru(CO)_3Cl(glycinate)$ (CORM-3) and CO probe 1 (COP-1) were prepared as described previously.[22,41] Recombinant L-chain apo-Fr from horse liver (rHLFr) was prepared in NovaBlue competent cells (Novagen) transformed with the expression vector pMK2 kindly supplied by Prof. Ichiro Yamashita. The culture and purification of the protein was performed according to a previous report.[46] Apo-R52C-rHLFr and apo-E45C/C48A-rHLFr mutants were prepared using a Stratagene Quikchange MultiSite kit.[28] The HEWL-CORM composite was synthesized following the previous report.[23] Sperm whale myoglobin which was used for myoglobin (Mb) assay was expressed and purified according to the reported procedure.[4] DMEM (Sigma, D5796) cell culture medium containing 5% FBS, 1.8 mM L-glutamine, 0.9 mM sodium pyruvate, 0.1% sodium bicarbonate, 1% MEM nonessential amino acid solution (Sigma, M7145), 90 U/mL penicillin, and 90 μg/mL streptomycin was used for cell culture.

Preparation of RuCO·apo-rHLFr (1). A DMF solution of $[Ru(CO)_3Cl_2]_2$ (CORM-2) (2.9 mM, 500 μL) was added to a buffer solution of recombinant L-chain apo-Fr from horse liver (apo-rHLFr, 5 μM, 10 mL in 50 mM Tris/HCl (pH 8.0), 0.15 M NaCl). The reaction mixture was incubated for 1 h at 50 °C. After the reaction, the solution was dialyzed against 50 mM Tris/HCl (pH 8.0), 0.15 M NaCl overnight at 4 °C. **1** was purified by size exclusion column chromatography (ÄKTA Design, Superdex G-200) equilibrated with 0.1 M sodium phosphate, pH 7.0. The concentrations of Ru atoms and protein of **1** were determined by ICP-MS and BCA assay, respectively. Same procedures were performed for RuCO·E45C/C48A-apo-rHLFr (**2**) and RuCO·R52C-apo-rHLFr (**3**).

Mb Assay. Mb assay was performed by the reported procedure.[47] All solutions for Mb assay were degassed by Ar bubbling for 30 min. **1** (180 μM Ru, 10 μL in 10 mM PBS buffer (pH 7.4)) was added to a solution of deoxy-Mb (7 μM, 90 μL in 10 mM PBS buffer (pH 7.4)) containing sodium dithionite (7 mM). Absorbance from 250 to 700 nm was recorded every 2 min after addition of **1**. Conversion of deoxy-Mb to MbCO was calculated according to the reported procedure.[22] The calculated data were fitted to first-order kinetics by using Microsoft Excel Solver.[48] The same assays and calculations for **1** were performed for **2**, **3**, and CORM-3 except for the initial concentration of CORM-3 (60 μM Ru, 10 μL in water) (Figure S1).

Reaction of 2 with Dithionite. **2** (120 μM Ru) was mixed with dithionite (17.3 mM) in 10 mM PBS buffer (pH 7.4). After incubation for 100 min at room temperature, excess dithionite was removed by a desalting column (HiTrap Desalting, GE Healthcare). The solution was used for GPC analysis (Figure S2).

Oxy-Hb Assay. The assay was performed following the previous report.[39] Bovine blood Hb (Sigma) (20 μM, in 10 mM PBS buffer (pH 7.4)) was reduced with dithionite (17.3 mM, in 10 mM PBS buffer (pH 7.4)). The mixture was purified by a desalting column (HiTrap Desalting, GE Healthcare) to obtain oxy-Hb with no residual dithionite. Oxy-Hb solution (6 μM, 100 μL) was bubbled with CO gas for 5 min to produce 100% Hb-CO. Oxy-Hb solution (6 μM, 100 μL) was mixed with **2** (Ru 60 μM, 10 μL) for 100 min. The absorbance spectra from 400 to 650 nm of the solutions were measured by UV–vis spectrometer (Figure S3).

Isolation of HEK293/κB-Fluc Cells. HEK293, a human embryonic kidney cell line, was purchased from the American Type Culture Collection. HEK293/κB-Fluc cells were isolated from a colony formed after transfection with pGL4/κB-luc2P plasmid by calcium phosphate method. pGL4/κB-luc2P plasmid was constructed as follows. First, pEF/HRE-luc2P was constructed by substituting the *Nco*I-*Xba*I fragment encoding luciferase in pEF/HRE-Luc with the *Nco*I-*Xba*I fragment encoding luc2P of pGL4.32 (Promega).[49] Next, pEF/κB-luc2P was constructed by substituting the *Xho*I-*Bgl*II fragment containing HRE sequences in pEF/HRE-luc2P with five tandem repeats of the NF-κB binding motif, which was prepared by annealing the following oligonucleotides: 5′-TCGAGGGGGACTTTCCGC-TTGGGGACTTTCCGCTGGGGACTTTC-3′, 5′-CGCTGGGG-ACTTTCCGCTGGGGACTTTCCGCA-3′, 5′-TCCCCAGCG-GAAAGTCCCCAAGCGGAAAGTCCCCC-3′, and 5′-ATCTGCGGAAAGTCCCCAGCGGAAAGTCCCCAGCGGAAAG-3′.[50]

Finally, *Kpn*I-*Eco*RI fragment containing κB-luc2P of pEF/κB-luc2P was inserted into *Kpn*I and *Eco*RI sites of pGL4.32 to obtain pGL4/κB-luc2P. The cells were cultured with Dulbecco's modified Eagle medium (Nacalai Tesque) supplemented with 5% fetal calf serum, penicillin (100 units/mL), and streptomycin (100 μg/mL) at 37 °C. Fluc reporter activity in HEK293/κB-Fluc cells in response to TNF-α treatments is shown in Supporting Information Figure S8.

ATTO520 Modification of 1. A DMSO solution of ATTO520-NHS-ester (ATTO-TEC, 120 μM) was added to an aqueous solution of **1** (5 μM in 0.1 M sodium phosphate (pH 7.0)). The mixture was

dx.doi.org/10.1021/ja508938f | J. Am. Chem. Soc. 2014, 136, 16902–16908

stirred at 25 °C for 12 h under the dark. ATTO-**1** was purified using Sephadex G-25 equilibrated with 0.1 M sodium phosphate (pH 7.0).

Confocal Imaging. HEK293/κB-Fluc cells were seeded into single-well glass-bottom dishes (1×10^5 cells/well) and incubated for 12 h at 37 °C under 5% CO_2. ATTO-**1** (30 μM, 10 μL in 0.1 M sodium phosphate (pH 7.0)) was added to the cells and incubated for 6 h. After the washing of the excess amounts of ATTO-**1** with 10 mM PBS buffer (pH 7.4), the images were observed (excitation, 488 nm; emission filter, 525/50) (Figure S4).

Cellular Uptake of Fr-CORM Composites and CORM-3. The intracellular uptake amount of Ru atoms determined by ICP-MS is described in a reported procedure.[22] HEK293/κB-Fluc cells were seeded in a six-well plate (2.0×10^5 cells/well) and incubated for 12 h at 37 °C under 5% CO_2. **1** (120 μM Ru, 100 μL in 0.1 M sodium phosphate (pH 7.0)) or CORM-3 (120 μM Ru, 100 μL in sterilized water) was added to the cultured cells in 1 mL of culture medium. After incubation for 12 h, the cells were collected as pellet by trypsinization and centrifugation. The pellet cells were washed with sterilized 10 mM PBS (pH 7.4) and centrifuged to obtain cell pellets. The pellets were lysed with 10% Tween 20 (50 μL). The concentration of Ru atoms in the cell lysate was measured by ICP-MS. The percentage of uptake was calculated from the amount of Ru atoms in culture medium and in the cell lysates using the following equation.

$$\text{uptake ratio (\%)} = \frac{[\text{find Ru in cell lysate}] \times \text{volume of cell lysate}}{[\text{find Ru in medium}] \times \text{volume of medium} + [\text{find Ru in cell lysate}] \times \text{volume of cell lysate}} \times 100$$

The same evaluations were done for **2**, **3**, and CORM-3.

Evaluation of Intracellular Stability of Fr Cage. HEK293/κB-Fluc cells were seeded into six-well plate (1×10^5 cells/well) with 1 mL of culture medium and incubated for 12 h at 37 °C under 5% CO_2. ATTO-**1** (3 μM, 100 μL in 0.1 M sodium phosphate (pH 7.0)) was added to the culture medium. After the incubation for 12 h, the cells were collected as pellet by trypsinization and centrifugation. The pellet cells were washed with sterilized 10 mM PBS (pH 7.4) twice and lysed by 10% Tween 20 (50 μL). The lysate was centrifuged to obtain a supernatant solution. The solution was used for GPC analysis (Figure S5).

Intracellular CO Imaging. HEK293/κB-Fluc cells were seeded into single-well glass-bottom dishes (3×10^4 cells/well) with 100 μL of phenol red-free medium and incubated for 48 h at 37 °C under 5% CO_2. **2** (200 μM or 1 mM Ru, 10 μL in 0.1 M sodium phosphate (pH 7.0)) was added to the culture medium and incubated for 60 min at 37 °C under 5% CO_2. After the removal of the medium, 1 μM COP-1 was added to the plate. The cells were incubated for 30 min at 37 °C under 5% CO_2 before imaging (excitation, 488 nm) (Figure S6).

Luciferase Assay. HEK293/κB- Fluc cells, which were applied in a luciferase reporter assay system, were cultured in 96-well plate (1×10^4 cells/well) with 100 μL of culture medium and incubated for 12 h at 37 °C under 5% CO_2. A solution of **1** (120 μM [Ru], 10 μL in 0.1 M sodium phosphate pH 7.0) was added to the cultured cells, and then the cells were incubated for 1 h. After the incubation, TNF-α (12 ng/mL, 10 μL in 0.1 M sodium phosphate, pH 7.0) was added to cultured cell and incubated for 12 h. Then the cells were treated with reagents (Promega, ONE-Glo luciferase assay system) to measure the luminescence corresponding to activity of NF-κB. The luminescence from the cells were measured with a 96-well plate reader. Same assays were performed for **2**, **3** (120 μM [Ru], 10 μL in 0.1 M sodium phosphate, pH 7.0), CORM-3 (120 μM [Ru], 10 μL in water), and HEWL-CORM (120 μM [Ru], 10 μL in water) composites (Figure 5 and Figure S6).

3-(4,5-Dimethylthiazol-2-yl)-2,5-diphenyltetrazolium Bromide (MTT) Assay. HEK293/κB-Fluc cells were seeded into 96-well plate (1×10^4 cells/well) and incubated for 12 h at 37 °C under 5% CO_2. A solution of **1** (120 μM Ru, 10 μL in 0.1 M sodium phosphate (pH 7.0)) or CORM-3 (120 μM Ru, 10 μL in sterilized water) was added to the cultured cells. After incubation for 12 h, a solution of MTT (Sigma, M5655) (10 μL) was added to each well and the cells were incubated for 4 h at 37 °C under 5% CO_2 to form formazan crystal. The formazan crystals were dissolved with a solution of DMSO (200 μL) after the removal of medium and washed with sterilized PBS (pH 7.4). A peak absorbance at 570 nm of formazan solution was measured using a 96-well plate reader (BIO-RAD, model 680 microplate reader). The same assay was performed for CORM-3 (Figure S7).

Statistical Analysis. Statistical analyses were carried out with a Student's *t* test. Values of $P < 0.05$ were considered statistically significant.

Physical Measurements. Absorption spectra were recorded on a UV-2400PC UV−vis spectrometer (Shimazu). ATR-IR measurements were conducted using a FT-IR4200 instrument (JASCO). Ru concentrations of Fr-CORM composites were determined by using an ICP-MS (PerkinElmer, Elan DRC-e instrument). A standard curve for Ru atom was obtained by using Ru standard solution (1 mg/mL Ru in 5% HCl) (Acros Organics, 196251000). Gel permeation chromatography (GPC) was carried out with a HPLC system and columns (Asahipack GF-510HQ, Shodex, Tokyo, Japan). Confocal imaging was conducted using a A1R confocal laser scanning microscope (Nikon). Luminescence measurements for luciferase assay were conducted using a GloMax-Multi plate reader (Promega). ^{1}H NMR (400 MHz) spectra were recorded with a Avance III (Bruker Biospin). ^{13}C NMR (500 MHz) spectra were recorded with a Avance III HD (Bruker Biospin). Fluorescence spectra were measured by using a F-7000 (Hitachi).

■ ASSOCIATED CONTENT

Ⓢ Supporting Information

Experimental procedures for X-ray crystallographic analysis, experimental results of Mb assay, stabilization of Fr cage reacted with dithionite, oxy-Hb assay, cellular uptake of Fr cage, stabilization of Fr cage in the cell, concentration-dependence luciferase assay, X-ray crystallographic data refinement statics, imaging by COP-1, viability and analyzed crystallographic data of Fr-CORM composites. This material is available free of charge via the Internet at http://pubs.acs.org.

■ AUTHOR INFORMATION

Corresponding Author

*tueno@bio.titech.ac.jp

Notes

The authors declare no competing financial interest.

■ ACKNOWLEDGMENTS

We thank the members of BL38B1 of SPring-8 for assistance during the diffraction data collection. Synchrotron radiation experiments were conducted under the approval of 2013B1262, 2013B1382 at SPring-8. Funding is from Next-Generation World-Leading Researchers (Grant LR019 to T.U.) from Ministry of Education, Culture, Sports, Science and Technology and from Tokuyama Science Foundation, Japan.

■ REFERENCES

(1) Vriezema, D. M.; Aragones, M. C.; Elemans, J. A. A. W.; Cornelissen, J. J. L. M.; Rowan, A. E.; Nolte, R. J. M. *Chem. Rev.* **2005**, *105*, 1445.

(2) Uchida, M.; Klem, M. T.; Allen, M.; Suci, P.; Flenniken, M.; Gillitzer, E.; Varpness, Z.; Liepold, L. O.; Young, M.; Douglas, T. *Adv. Mater.* **2007**, *19*, 1025.

(3) Ueno, T.; Watanabe, Y. *Coordination Chemistry in Protein Cages: Principles, Design, and Applications*; John Wiley and Sons: Hoboken, NJ, 2013.
(4) Ueno, T.; Tabe, H.; Tanaka, Y. *Chem.—Asian J.* **2013**, *8*, 1646.
(5) Liu, X.; Wei, W.; Wang, C.; Yue, H.; Ma, D.; Zhu, C.; Ma, G.; Du, Y. *J. Mater. Chem.* **2011**, *21*, 7105.
(6) Singh, P.; Prasuhn, D.; Yeh, R. M.; Destito, G.; Rae, C. S.; Osborn, K.; Finn, M. G.; Manchester, M. *J. Controlled Release* **2007**, *120*, 41.
(7) Brasch, M.; de la Escosura, A.; Ma, Y.; Uetrecht, C.; Heck, A. J.; Torres, T.; Cornelissen, J. J. *J. Am. Chem. Soc.* **2011**, *133*, 6878.
(8) Yang, Z.; Wang, X.; Diao, H.; Zhang, J.; Li, H.; Sun, H.; Guo, Z. *Chem. Commun.* **2007**, 3453.
(9) Geninatti Crich, S.; Bussolati, B.; Tei, L.; Grange, C.; Esposito, G.; Lanzardo, S.; Camussi, G.; Aime, S. *Cancer Res.* **2006**, *66*, 9196.
(10) Farkas, M. E.; Aanei, I. L.; Behrens, C. R.; Tong, G. J.; Murphy, S. T.; O'Neil, J. P.; Francis, M. B. *Mol. Pharmaceutics* **2013**, *10*, 69.
(11) Zhang, L.; Laug, L.; Munchgesang, W.; Pippel, E.; Gosele, U.; Brandsch, M.; Knez, M. *Nano Lett.* **2010**, *10*, 219.
(12) Uchida, M.; Flenniken, M. L.; Allen, M.; Willits, D. A.; Crowley, B. E.; Brumfield, S.; Willis, A. F.; Jacliw, L.; Jutila, M.; Young, M. J.; Douglas, T. *J. Am. Chem. Soc.* **2006**, *128*, 16626.
(13) Ma, Y.; Nolte, R. J.; Cornelissen, J. J. *Adv. Drug Delivery Rev.* **2012**, *64*, 811.
(14) Liu, X.; Wei, W.; Yuan, Q.; Zhang, X.; Li, N.; Du, Y.; Ma, G.; Yan, C.; Ma, D. *Chem. Commun.* **2012**, *48*, 3155.
(15) Hillard, E. A.; Jaouen, G. *Organometallics* **2011**, *30*, 20.
(16) Sasmal, P. K.; Streu, C. N.; Meggers, E. *Chem. Commun.* **2013**, *49*, 1581.
(17) Alberto, R.; Motterlini, R. *Dalton Trans.* **2007**, 1651.
(18) Mann, B. E. *Organometallics* **2012**, *31*, 5728.
(19) Romão, C. C.; Blattler, W. A.; Seixas, J. D.; Bernardes, G. J. *Chem. Soc. Rev.* **2012**, *41*, 3571.
(20) Motterlini, R.; Otterbein, L. E. *Nat. Rev. Drug Discovery* **2010**, *9*, 728.
(21) Johnson, T. R.; Mann, B. E.; Teasdale, I. P.; Adams, H.; Foresti, R.; Green, C. J.; Motterlini, R. *Dalton Trans.* **2007**, 1500.
(22) Hasegawa, U.; Vilies, A. J.; Simeoni, E.; Wandrey, C.; Hubbell, J. A. *J. Am. Chem. Soc.* **2010**, *132*, 18273.
(23) Santos-Silva, T.; Mukhopadhyay, A.; Seixas, J. D.; Bernardes, G. J.; Romão, C. C.; Romão, M. J. *J. Am. Chem. Soc.* **2011**, *133*, 1192.
(24) Santos, M. F.; Seixas, J. D.; Coelho, A. C.; Mukhopadhyay, A.; Reis, P. M.; Romão, M. J.; Romão, C. C.; Santos-Silva, T. *J. Inorg. Biochem.* **2012**, *117*, 285.
(25) Theil, E. C. *Curr. Opin. Chem. Biol.* **2011**, *15*, 304.
(26) Abe, S.; Niemeyer, J.; Abe, M.; Takezawa, Y.; Ueno, T.; Hikage, T.; Erker, G.; Watanabe, Y. *J. Am. Chem. Soc.* **2008**, *130*, 10512.
(27) Wang, Z.; Takezawa, Y.; Aoyagi, H.; Abe, S.; Hikage, T.; Watanabe, Y.; Kitagawa, S.; Ueno, T. *Chem. Commun.* **2011**, *47*, 170.
(28) Takezawa, Y.; Bockmann, P.; Sugi, N.; Wang, Z.; Abe, S.; Hikage, T.; Erker, G.; Watanabe, Y.; Kitagawa, S.; Ueno, T. *Dalton Trans.* **2011**, *40*, 2190.
(29) Abe, S.; Hikage, T.; Watanabe, Y.; Kitagawa, S.; Ueno, T. *Inorg. Chem.* **2010**, *49*, 6967.
(30) Abe, S.; Hirata, K.; Ueno, T.; Morino, K.; Shimizu, N.; Yamamoto, M.; Tanaka, M.; Yashima, E.; Watanabe, Y. *J. Am. Chem. Soc.* **2009**, *131*, 6958.
(31) Caamano, J.; Hunter, C. A. *Clin. Microbiol. Rev.* **2002**, *15*, 414.
(32) Lai, Y.-H.; Chen, Y.-L.; Chi, Y.; Liu, C.-S.; Carty, A. J.; Peng, S.-M.; Lee, G.-H. *J. Mater. Chem.* **2003**, *13*, 1999.
(33) Shiu, K.-B.; Yu, S.-J.; Wang, Y.; Lee, G.-H. *J. Organomet. Chem.* **2002**, *650*, 37.
(34) Hempstead, P. D.; Yewdall, S. J.; Fernie, A. R.; Lawson, D. M.; Artymiuk, P. J.; Rice, D. W.; Ford, G. C.; Harrison, P. M. *J. Mol. Biol.* **1997**, *268*, 424.
(35) Ueno, T.; Abe, M.; Hirata, K.; Abe, S.; Suzuki, M.; Shimizu, N.; Yamamoto, M.; Takata, M.; Watanabe, Y. *J. Am. Chem. Soc.* **2009**, *131*, 5094.
(36) Wang, P.; Liu, H.; Zhao, Q.; Chen, Y.; Liu, B.; Zhang, B.; Zheng, Q. *Eur. J. Med. Chem.* **2014**, *74*, 199.
(37) Adams, R. D.; Babin, J. E.; Tasi, M. *Inorg. Chem.* **1986**, *26*, 2561.
(38) McLean, S.; Mann, B. E.; Poole, R. K. *Anal. Biochem.* **2012**, *427*, 36.
(39) Li, J. Y.; Paragas, N.; Ned, R. M.; Qiu, A.; Viltard, M.; Leete, T.; Drexler, I. R.; Chen, X.; Sanna-Cherchi, S.; Mohammed, F.; Williams, D.; Lin, C. S.; Schmidt-Ott, K. M.; Andrews, N. C.; Barasch, J. *Dev. Cell* **2009**, *16*, 35.
(40) Xing, R.; Wang, X.; Zhang, C.; Zhang, Y.; Wang, Q.; Yang, Z.; Guo, Z. *J. Inorg. Biochem.* **2009**, *103*, 1039.
(41) Michel, B. W.; Lippert, A. R.; Chang, C. J. *J. Am. Chem. Soc.* **2012**, *134*, 15668.
(42) Kim, H. S.; Loughran, P. A.; Rao, J.; Billiar, T. R.; Zuckerbraun, B. S. *Am. J. Physiol.: Gastrointest. Liver Physiol.* **2008**, *295*, G146.
(43) Ueno, T.; Suzuki, M.; Goto, T.; Matsumoto, T.; Nagayama, K.; Watanabe, Y. *Angew. Chem., Int. Ed.* **2004**, *116*, 2581.
(44) Zobi, F. *Inorg. Chem.* **2010**, *49*, 10370.
(45) Ragin, A. D.; Morgan, R. A.; Chmielewski. *J. Chem. Biol.* **2002**, *8*, 943.
(46) Iwahori, K.; Yoshizawa, K.; Muraoka, M.; Yamashita, I. *Inorg. Chem.* **2005**, *44*, 6393.
(47) Motterlini, R. *Circ. Res.* **2002**, *90*, 17e.
(48) Hewison, L.; Crook, S. H.; Mann, B. E.; Meijer, A. J. H. M.; Adams, H.; Sawle, P.; Motterlini, R. A. *Organometallics* **2012**, *31*, 5823.
(49) Kizaka-Kondoh, S.; Itasaka, S.; Zeng, L.; Tanaka, S.; Zhao, T.; Takahashi, Y.; Shibuya, K.; Hirota, K.; Semenza, G. L.; Hiraoka, M. *Clin. Cancer Res.* **2009**, *15*, 3433.
(50) Sen, R.; Baltimore, D. *Cell* **1986**, *46*, 705.